Quantitative Electrochemical and Electrochromic Behavior of Terthiophene and Carbazole Containing Conjugated Polymer Network Film Precursors: EC-QCM and EC-SPR

Prasad Taranekar, Timothy Fulghum, Akira Baba, Derek Patton, and Rigoberto Advincula*

Department of Chemistry and Department of Chemical Engineering, University of Houston, Houston, Texas 77204-5003

Received June 23, 2006. In Final Form: September 28, 2006

A comparative analysis of the copolymerization behavior between an electro-active terthiophene and a carbazole moiety of a conjugated polymer precursor was investigated using electrochemical and hyphenated electrochemical methods. Five different precursor polymers were first synthesized and characterized using NMR, IR, and GPC. The polymers include homopolymers of individual electro-active groups (P3T, P−CBZ) and different compositions of 25, 50, and 75% (P3TC-25, P3TC50, and P3TC-75) with respect to the two electro-active groups. Since the oxidation potentials of terthiophene and carbazole lie very close to each other, highly cross-linked copolymer films of varying extent were produced depending on the composition. The copolymerization extent was found to be dependent primarily on the amount of the terthiophene, which in this case provided for a more efficient carbazole polymerization and copolymerization than with just carbazole alone (homopolymer). The extent of copolymerization, electrochromic properties, and viscoelastic changes was quantitatively investigated using a number of hyphenated electrochemistry techniques: spectro-electrochemistry, electrochemical quartz crystal microbalance studies (EC-QCM), and electrochemical surface plasmon resonance spectroscopy (EC−SPR). Each technique revealed a unique aspect of the electrocopolymerization behavior that was used to define structure−property relationships and the deposition/copolymerization mechanism.

Introduction

Over the past several decades, conjugated polymers have been investigated in terms of their preparation, properties, and characterization.[1] The potential applications include their use as sensors,[2] electro-optical materials,[2b] and semiconducting devices.[3] A large number of applications exist based on electrochromism, which relies on the reproducible switching characteristics of conjugated polymers.[4] In particular, thiophene and carbazole copolymers have been of recent interest due to their interesting electrochemical copolymerization behavior[5] and electrochromic properties.[6] It has been shown in the past that electropolymerization of terthiophene leads to the formation of highly electrochromic and conducting polythiophenes.[7] On the other hand, polycarbazole is well-known as a hole transport material.[8] Furthermore, electrochemically polymerized carbazoles show interesting chromic properties because of the conjugation breaks that are present due to the inclusion of a 3,6-linkage. These broken conjugation lengths generate radical cations, which are separated from one another and do not combine. Therefore, the ability of polycarbazole to form two distinct oxidation states further leads to multichromic effects.[9]

Electrochemical oxidative polymerization has been widely utilized to precisely control the polymerization of electro-active monomers and to study the resulting electronic properties. Typically, electrochemical polymerization entails oxidative coupling of monomers in a stepwise manner to produce insoluble oligomers that deposit (precipitate) onto the working electrode surface. Oftentimes, because of the rigid character of the resulting polymers, they are intractable and insoluble in many common organic solvents, thereby leading to major difficulties in film processing.[10] By far, the most common method for obtaining organic soluble conjugated polymers is to introduce alkyl side chains. Recently, the Advincula group has focused on a precursor polymer route in which the alkyl substituted electro-active monomers were tethered to a desired polymer backbone.[11] The precursor approach is highly advantageous in terms of its versatility in utilizing the polymer backbone, which is useful in many ways such as imparting thermal stability/flexibility, adhesion, morphological modification, optical transparency, and

(1) (a) Li, Y.; Vamvounis, G.; Holdcroft, S. *Macromolecules* **2002**, *35*, 6900−6906. (b) Fukukawa, K.; Shibasaki, Y.; Ueda, M. *Macromolecules* **2004**, *37*, 8256−8261. (c) Katz, H. E. *Chem. Mater.* **2004**, *16*, 4748−4756. (d) Kraft, A.; Grimsdale, A. C.; Holmes, A. B. *Angew. Chem., Int. Ed.* **1998**, *37*, 402−428. (e) Friend, R. H.; Gymer, R. W.; Holmes, A. B.; Burroughes, J. H.; Marks, R. N.; Taliani, C.; Bradley, D. D. C.; Dos Santos, D. A.; Brédas, J. L.; Lögdlund, M.; Salaneck, W. R. *Nature* **1999**, *397*, 121−127.

(2) (a) Wang, X.; Kim, Y.-G.; Drew, C.; Ku, B.-C.; Kumar, J.; Samuelson, L. A. *Nano Lett.* **2004**, *4* (2), 331−334. (b) Tong, H.; Wang, L.; Jing, X.; Wang, F. *Macromolecules* **2003**, *36* (8), 2584−2586. (c) Murphy, C. B.; Zhang, Y.; Troxler, T.; Ferry, V.; Martin, J. J.; Jones, W. E., Jr. *J. Phys. Chem. B* **2004**, *108* (5), 1537−1543.

(3) Dodabalapur, A.; Torsi, L.; Katz, H. E. *Science* **1995**, *268*, 270−271.

(4) (a) Sonmez, G.; Sonmez, H. B.; Shen, C. K. F.; Jost, R. W.; Rubin, Y.; Wudl, F. *Macromolecules* **2005**, 38, 669−675. (b) Nadeau, J. M.; Swager, T. M. *Tetrahedron* **2004**, 60, 7141−7146. (c) Gao, J.; Liu, D.-G.; Sansinena, J. M.; Wang, H. L. *Adv. Funct. Mater.* **2004**, *14*, 537−543. (d) DuBois, C. J.; Abboud, K. A.; Reynolds, J. R. *J. Phys. Chem. B* **2004**, *108*, 8550−8557.

(5) Taranekar, P.; Baba, A.; Fulghum, T.; Advincula, R. *Macromolecules* **2005**, *38* (9), 3679−3687.

(6) (a) Witker, D.; Reynolds, J. R. *Macromolecules* **2005**, *38* (18), 7636−7644. (b) Gaupp, C. L.; Reynolds, J. R. *Macromolecules* **2003**, *36* (17), 6305−6315.

(7) (a) Jang, S.-Y.; Sotzing, G. A. *Macromolecules* **2004**, *37*, 4351−4359. (b) Zotti, G.; Marin, R. A.; Gallazzi, M. C. *Chem. Mater.* **1997**, *9* (12), 2945−2950. (c) Jang, S.-Y.; Sotzing, G. A.; Marquez, M. *Macromolecules* **2002**, *35* (19), 7293−7300. (d) DiCesare, N.; Belletete, M.; Marrano, C.; Leclerc, M.; Durocher, G. *J. Phys. Chem. A* **1999**, *103* (7), 795−802.

(8) Baba, A.; Onishi, K.; Knoll, W.; Advincula, R. C. *J. Phys. Chem. B* **2004**, *108* (49), 18949−18955.

(9) (a) Gaupp, C. L.; Reynolds, J. R. *Macromolecules* **2003**, *36*, 6305−6315. (b) Sotzing, G. A.; Reddinger, J. L.; Katritzky, A. R.; Soloducho, J.; Musgrave, R.; Reynolds, J. R. *Chem. Mater.* **1997**, *9*, 1578−1587. (c) Reddinger, J. L.; Sotzing, G. A.; Reynolds, J. R. *Chem. Commun.* **1996**, *15*, 1777−1778.

(10) Skotheim, T. A.; Elsenbaumer, R. L.; Reynolds, J. R. *Handbook of Conducting Polymers*, 2nd ed.; Marcel Dekker: New York, 1998.

(11) (a) Taranekar, P.; Fan, X.; Advincula, R. *Langmuir* **2002**, *18*, 7943−7952. (b) Xia, C.; Fan, X.; Park, M.; Advincula, R. *Langmuir* **2001**, *17*, 7893−7898. (c) Deng, S.; Advincula, R. C. *Chem. Mater.* **2002**, *14* (10), 4073−4080.

10.1021/la061820d CCC: $37.00
Published on Web 12/05/2006

controlling ion permeability. Besides, one can also retain and even tune the alkyl side chain length, which helps modulate the electronic properties of the conjugated main chain. In the past, for example, a thermoplastic polymethacrylate (PMMA) polymer precursor was chosen to produce polypyrrole films of high optical quality and morphological smoothness.[11c]

Although a number of investigations have focused on chemically copolymerizing conjugated polymers, very little attention has been given to methods or ways to systematically study electrochemical copolymerization phenomena. The use of precursor polymers permits fundamental studies of controlling the copolymerization within two electro-active species in a compositionally controlled manner. Thus, the electrochemical method not only eliminates the need for rigorous synthesis but may allow one to easily generate films of desired composition, thickness, and controlled morphology directly on the conducting substrate for practical applications.[5,11a]

In this paper, precursor polymers that contain two pendent electro-active monomer units by design were investigated for their copolymerization phenomena in forming conjugated polymer network films. Terthiophene and carbazole were chosen as electro-active components because their redox window lies very close to each other. They should effectively undergo very good statistical copolymerization under controlled electrochemical conditions because of a similar reactivity. The resulting polymers then exhibited electrochromic behavior. Thus, statistical precursor copolymers were synthesized having different composition ratios (25, 50, and 75%) with respect to the monomer units including the individual precursor homopolymers (P3T and P−CBZ) to differentiate electrocopolymerization and homopolymer electropolymerization behavior. The cyclic voltammetry (CV) technique was mainly used to generate the cross-linked polymers. The polymers were found to show electrochromism accompanied by changes in the physical/chemical characteristics of the film affecting the optoelectronic, mass, viscoelastic effects, and dielectric constant properties. These changes were monitored using electrochemistry methods such as spectro-electrochemistry, in situ electrochemical surface plasmon resonance spectroscopy (EC−SPR), and in situ electrochemical quartz crystal microbalance (EC-QCM) studies. Such electrochemical and optical quantitative analyses in π conjugated polymers during the oxidation/reduction or doping−de-doping are not only very useful for probing the changes in properties but should also hold promise for monitoring real time changes in a number of device and sensor applications.

Experimental Procedures

Instrumentation. NMR spectra were recorded using a General Electric QE 300 spectrometer (^{1}H 300 MHz). UV−vis spectra were recorded using an Agilent 8453 spectrometer. The SEC analysis was performed using a Viscotek 270 quad detector equipped with a VE3210 UV−vIS detector and VE3580 RI detector. The columns used for finding size exclusion chromatography (SEC) number-average molecular weight (M_{nsec}) types were G3000H_{HR} and GHM_{HR}-M Viscogel. All FTIR measurements were performed using a Digilab FTS 7000 step scan spectrometer. Cyclic voltammetry was performed on an Amel 2049 potentiostat and power lab/4SP system with a three-electrode cell. In all the measurements, the counter electrode was platinum wire, and indium tin oxide (ITO) or gold-coated glass was used as a working electrode. The ITO was pretreated with the RCA recipe ($H_2O/H_2O_2/NH_3$: 15.1 g/26.6 g/8.57 g).[12] The gold electrodes were cleaned with a plasma ion cleaner (Plasmod, March). The QCM apparatus, probe, and crystals are

Scheme 1. Synthesis of Monomers

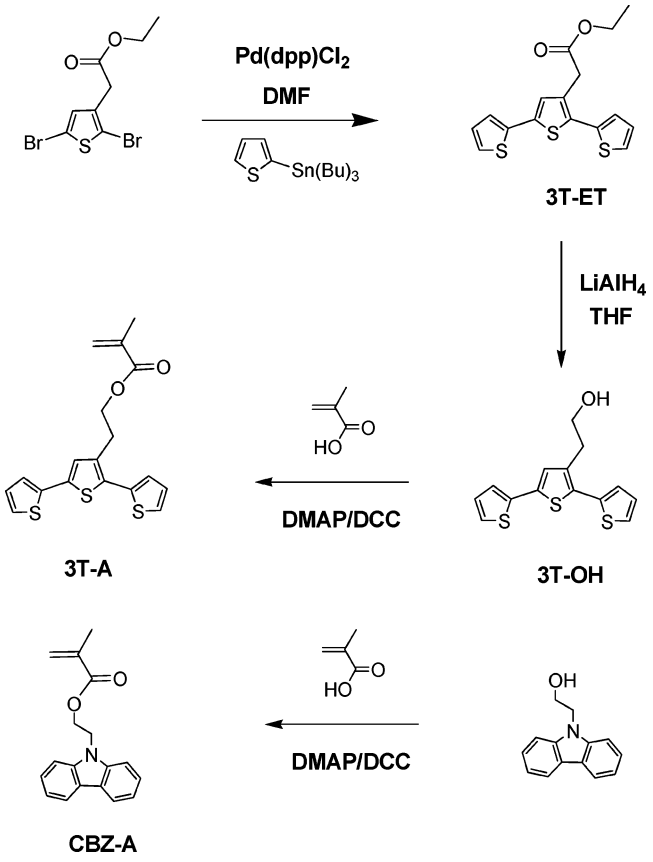

available from MAXTEK Inc. The data acquisition was done using a RQCM (Research Quartz Crystal Microbalance, MAXTEK, Inc.) system equipped with a built-in phase lock oscillator and the RQCM Data-Log Software. This was coupled with the Amel potentiostat to generate EC-QCM results. A 5 MHz AT-cut Au-coated quartz crystal with an effective area of 1.327 cm^2 was used as a working electrode. Platinum as a counter electrode and Ag/AgCl as a reference were used to measure in situ polymerization during cyclic voltammetry. To initiate the experiment, an inert probe was first immersed in methylene chloride until a stable frequency was obtained.

Electrochemical surface plasmon resonance spectroscopy (EC−SPR) measurements were performed using a surface plasmon resonance (SPR) setup combined with a three-electrode electrochemical cell in a Kretschmann configuration for the excitation of surface plasmons. The details of this setup are described elsewhere.[13] Surface plasmons are excited by reflecting *p*-polarized laser light off the Au-coated base of the prism. The excitation source employed was a He−Ne laser: $\lambda = 632.8$ nm. Kinetic measurements were performed to monitor the formation of the film and the oxidation/reduction and doping/de-doping properties of a deposited polycarbazole thin film via reflectivity changes as a function of time. Reflectivity−angular measurements were also performed by scanning an incident angle range while the potential was held constant. For these experiments, the gold film thickness (∼45 nm) was chosen for optimum excitation of the surface plasmons. The electrode surface area was 0.785 cm^2.

Reagents. All the chemicals were purchased from Aldrich. Distilled and properly dried solvent were used for all the measurements including synthesis.

Synthesis of Ethyl 2-(2,5-Di(thiophen-2-yl)thiophen-3-yl)-acetate (3T-ET) [Scheme 1]. The synthesis of 3T-ET was carried by first synthesizing ethyl 2-(2,5-dibromothiophen-3-yl)acetate as reported in the literature.[14] The same literature procedure was

(12) Magnus, P.; Friend, R.; Greenham, N. *Adv. Mater.* **1998**, *10* (10), 769−774.

(13) Knoll, W. *Annu. Rev. Phys. Chem.* **1998**, *49*, 569−638.

(14) Yassar, A.; Moustrou, C.; Youssoufi, H. K.; Samat, A.; Guglielmetti, R.; Garnier, F. *Macromolecules* **1995**, *28*, 4548−4553.

Scheme 2. Synthesis of Precursor Homopolymers/Copolymers and Their Electropolymerization

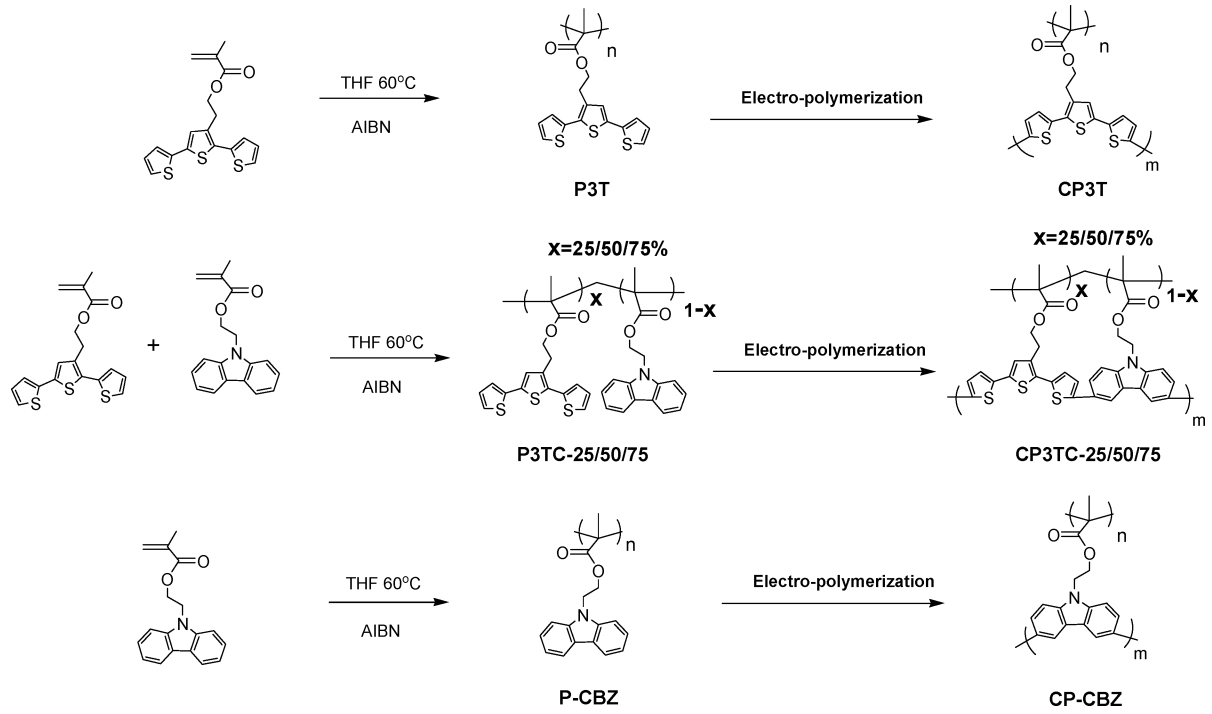

modified to synthesize 3T-ET. Ethyl 2-(2,5-dibromothiophen-3-yl)acetate (6.4 g, 10 mmol) and 2-(tributylstanny1) thiophene (15 g, 20 mmol) were added to a 30 mL dry DMF solution of dichlorobis-(tripheny1phosphine)palladium (1.3 g, 1.5 mmol). After three freeze−thaw cycles, the mixture was heated at 100 °C for 48 h. The mixture was cooled to room temperature and poured into a beaker containing 150 mL of water and subsequently extracted with CH_2Cl_2. The extracted CH_2Cl_2 mixture was dried with Na_2SO_4. After filtering and evaporation of solvent, the crude product was purified by chromatography on silica gel using toluene as an eluent. The final product was obtained in 85% yield as pale yellow oil. The characterization of the compound was found in accordance with the literature.

Synthesis of 2-(2,5-Di(thiophen-2-yl)thiophen-3-yl)ethanol (3T-OH) [Scheme 1]. The compound 3T-ET (2 g, 5.9 mmol) in 10 mL of THF was dropwise added under nitrogen to an ice cooled 100 mL THF suspension of (0.32 g, 8.4 mmol) $LiAlH_4$. Upon addition, the color of the solution immediately turned red. After complete addition, the ice bath was removed, the reaction was allowed to warm to room temperature, and constant stirring was maintained for 12 h. The reaction was quenched by adding water and neutralized by a 2 N HCl solution. The red solution immediately turned yellow upon neutralization. The solvent was evaporated, and the resulting mixture was extracted three times using CH_2Cl_2. The combined CH_2Cl_2 extract was again washed with water, brine, and dried with Na_2SO_4. After filtering and evaporating CH_2Cl_2, the reaction mixture was chromatographed using (4:1) CH_2Cl_2/hexane as an eluent mixture. The final product was obtained in 90% yield as oil, which solidified upon vacuum or even at room temperature if kept for a longer time. ^{1}H NMR in $CDCl_3$ (δ ppm): 7.31−7.04 (m, 7H), 3.88 (q, 2H, J = 6.4 Hz), 3.01 (t, 2H, J = 6.4 Hz). ^{13}C NMR: 136.8, 135.8, 135.7, 135.2, 131.2, 127.8, 127.5, 126.4, 126.3, 125.7, 124.6, 123.8, 62.7, 32.4.

Synthesis of 2-(2,5-Di(thiophen-2-yl)thiophen-3-yl)ethyl Methacrylate (3T-A) [Scheme 1]. A 5 mL solution of dicyclohexylcarbodiimide (DCC) (1.96 g, 9.5 mmol) in CH_2Cl_2 was added dropwise under nitrogen to an ice cooled CH_2Cl_2 solution (15 mL) containing methacrylic acid (0.7 g, 8.2 mmol), 3T-OH (2 g, 6.8 mmol), and a catalytic amount of *p*-(dimethylamino)pyridine (0.12 g, 0.96 mmol). Upon complete addition of DCC, the cooling bath was removed, and the reaction was allowed to stir at room temperature for 24 h. The byproduct dicyclohexylurea was removed by filtration, and the solvent was removed by rotary evaporation. The resulting residue was purified by column chromatography on silica gel using (3:1) *n*-hexane/CH_2Cl_2. The pure product was obtained as yellowish oil in 74% yield. ^{1}H NMR in $CDCl_3$ (δ ppm): 7.34−7.04 (m, 7H), 6.09 (b, 1H), 5.56 (b, 1H), 4.39 (t, 2H, J = 6.9 Hz), 3.13 (t, 2H, J = 6.9 Hz), 1.94 (s, 3H). ^{13}C NMR: 167.3, 136.8, 136.2, 135.7, 135.1, 135.0, 131.1, 127.8, 127.6, 126.43, 126.4, 125.8, 125.7, 124.5, 123.7, 64.2, 28.4, 18.3.

Synthesis of 2-(9H-Carbazol-9-yl)ethyl Methacrylate (CBZ-A) [Scheme 1]. CBZ-A was synthesized using commercially available 2-(9H-carbazol-9-yl)ethanol and following the procedure in same molar ratios as described for compound 3T−A. The pure product was obtained in 86% yield as white fluffy solid. ^{1}H NMR in $CDCl_3$ (δ ppm): 8.12 (d, 2H, J = 7.5 Hz), 7.51−7.44 (m, 4H), 7.24−7.23 (m, 2H), 5.94 (b, 1H), 5.49 (m, 1H), 4.64−4.22 (m, 4H), 1.82 (s, 3H). ^{13}C NMR: 167.2, 140.3, 135.6, 126.3, 125.7, 122.9 120.3, 119.2, 108.5, 62.4, 41.5, 18.2.

Synthesis of Poly[2-(9H-carbazol-9-yl)ethyl Methacrylate] (P−CBZ) [Scheme 2]. A 50 mL Schlenk flask containing 0.58 g (2.04 mmol) of CBZ-A and 34 mg (0.2 mmol) of azobisisobutyronitrile (AIBN) in 7 mL of THF was subjected to four freeze−degas−thaw cycles and sealed under vacuum. Polymerization was run in bulk at 60 °C for 18 h. The resulting slurry was dropwise added to hexane, and the cloudy solution was centrifuged at 4500 rpm for 5 min. The supernatant was discarded, and the precipitated polymer was redissolved, precipitated, and centrifuged again. The precipitation redispersion cycle was performed up to 5 times. The precipitated polymer was collected by filtration and dried in a vacuum oven at 45 °C for 72 h. The polymer was obtained in 93.1% yield as a white powder. ^{1}H NMR in $CDCl_3$ (δ ppm): 7.93 (b, 2H), 7.25−7.09 (b, 6H), 4.18−3.98 (b, 4H), 1.6−1.39 (b, 2H), 0.14−0.19 (b, 3H). The FTIR (KBr) in wavenumber (cm^{-1}) shows[15] out of plane deformation (C−H) 701−754(s), (CH_3−polymer backbone) 1160−1180(m), (C−O) 1190−1200(s), $(C-N)_{ring}$ 1217(s), carbazole aromatic (C−H) 1470−1525(s), carbazole $(C{=}C)_{ring}$ 1590−1622-(s), ester (C═O) 1728 (s), $\upsilon_s(CH_2)$ 2860(br), υ(CH) 2910(br), υ_{as}-(CH_2) 2932(br).

(15) (a) Colthup, N. B. *Introduction to Infrared and Raman Spectroscopy*, 2nd ed.; Academic Press: New York, 1975. (b) Mangeney, C.; Lacroix, J.-C.; Chane-Ching, K. I.; Jouini, M.; Villain, F.; Ammar, S.; Jouini, N.; Lacaze, P.-C. *Chem.−Eur. J.* **2001**, *7* (23), 5029−5040.

Synthesis of Poly[2-(2,5-di(thiophen-2-yl)thiophen-3-yl)ethyl Methacrylate] (P-3T) [Scheme 2]. P3T was synthesized following the procedure of P-CBZ. A molar ratio of 0.75 g (2.04 mmol) of 3T-A and 34 mg (0.2 mmol) of AIBN in 7 mL of THF was used. The polymer was obtained in 73.3% yield as a pale yellow powder. ^{1}H NMR in $CDCl_3$ (δ ppm): 7.26−6.88 (b, 7H), 4.02 (b, 2H), 2.90 (b, 2H), 1.78−1.59 (b, 2H), 0.89−0.31 (b, 3H). The FTIR (KBr) in wavenumber (cm^{-1}) shows[15] out of plane deformation (C−H) 701−754(s), out of plane $(C_\beta\text{-H})_{ring}$ 817−839(br, s), (CH_3−polymer backbone) 1160−1180(m), (C−O) 1190−1200(s), (C═O) 1728 overlapped with thiophene $(C{=}C)_{ring}$ 1736(b), $\upsilon_s(CH_2)$ 2860(br), υ(CH) 2910(br), $\upsilon_{as}(CH_2)$ 2932(br).

Synthesis of the Poly[(2-{2,5-di(thiophen-2-yl)thiophen-3-yl}-ethyl-*co*-(2-{9H-carbazol-9-yl}ethyl Methacrylate] (25:75 mol %, P3TC-25) [Scheme 2]. The random copolymer was synthesized using the procedure that was described earlier and weighing 0.18 g (0.5 mmol) of 3T-A, 0.42 g (1.5 mmol) of CBZ-A, and 34 mg (0.2 mmol) of AIBN in 7 mL of THF. The polymer was obtained in 89% yield as a white powder. ^{1}H NMR in $CDCl_3$ (δ ppm): 7.96 (b, 1.5H), 7.25−6.90 (b, 8H), 4.21−3.99 (b, 4H), 2.88 (b, 0.35H), 1.62−1.41 (b, 2H), 0.14−0.19 (b, 3H). The FTIR (KBr) in wavenumber (cm^{-1}) shows[15] out of plane $(C_\beta{-}H)_{ring}$ 817−839(br, w), $(C{-}N)_{ring}$ 1217-(s), carbazole aromatic (C−H) 1470−1525(s), carbazole $(C{=}C)_{ring}$ 1590(s), ester (C═O) 1728 overlapped with thiophene $(C{=}C)_{ring}$ 1736(s).

Synthesis of the Poly[(2-{2,5-di(thiophen-2-yl)thiophen-3-yl}-ethyl-*co*-(2-{9H-carbazol-9-yl}ethyl Methacrylate] (50:50 mol %, P3TC-50) [Scheme 2]. The random copolymer was also synthesized following same procedure as described earlier using 375 mg (1.01 mmol) of 3T-A, 290 mg (1.01 mmol) of CBZ-A, and 34 mg (0.2 mmol) of AIBN in 7 mL of THF. The polymer was obtained in 82% yield as an off-white powder. ^{1}H NMR in $CDCl_3$ (δ ppm): 7.98 (b, 1.02H), 7.25−6.88 (b, 9H), 4.24−4.01 (b, 4H), 2.88 (b, 0.77H), 1.62−1.41 (b, 2H), 0.58−0.25 (b, 3H). The FTIR (KBr) in wavenumbers (cm^{-1}) shows[15] out of plane $(C_\beta{-}H)_{ring}$ 817−839(br, m), $(C{-}N)_{ring}$ 1217(m), carbazole aromatic (C−H) 1470−1525(m), carbazole $(C{=}C)_{ring}$ 1590(m), ester (C═O) 1728 overlapped with thiophene $(C{=}C)_{ring}$ 1736(b, m).

Synthesis of the Poly[(2-{2,5-di(thiophen-2-yl)thiophen-3-yl}-ethyl-*co*-(2-{9H-carbazol-9-yl}ethyl Methacrylate] (75:25 mol %, P3TC-75) [Scheme 2]. A similar procedure as described earlier was used to synthesize P3TC-75 using 0.54 g (1.5 mmol) of 3T-A, 0.14 g (0.5 mmol) of CBZ-A, and 34 mg (0.2 mmol) of AIBN in 7 mL of THF. The polymer was obtained in 79.8% yield as a beige powder. ^{1}H NMR in $CDCl_3$ (δ ppm): 7.98 (b, 0.39H), 7.29−6.89 (b, 9H), 4.33−4.03 (b, 3H), 2.89 (b, 1.26H), 1.75−1.58 (b, 2H), 0.88−0.30 (b, 3H). The FTIR (KBr) in wavenumbers (cm^{-1}) shows[15] out of plane $(C_\beta{-}H)_{ring}$ 817−839(br, s), $(C{-}N)_{ring}$ 1217(w), carbazole aromatic (C−H) 1470−1525(w), carbazole $(C{=}C)_{ring}$ 1590(w), ester (C═O) 1728 overlapped with thiophene $(C{=}C)_{ring}$ 1736(b, w).

Electrochemical Synthesis of Cross-Linked Polymers (P-CBZ/P3TC-25/P3TC-50/P3TC-75/P3T). The precursor polymers were electropolymerized using the cyclic voltammetry (CV) technique. In a three-electrode cell, 0.1 M tetra-butylammonium perchlorate (TBAP) was taken as a supporting electrolyte along with 5 mM each polymer dissolved in 6 mL of methylene chloride in separate cells. The electropolymerization of each precursor polymer was performed by sweeping the voltage at a scan rate of 20 mV/s from 0 to 1.2 V against Ag/AgCl as a reference electrode and platinum as a counter electrode. The ITO or gold-coated slides were used as a working electrode and also as a substrate.

Results and Discussion

The homopolymers (P-CBZ and P3T) and the statistical copolymers with different compositions (P3TC-25/50/75) were synthesized via free radical polymerization using AIBN as an initiator. The polymers were characterized using NMR, FT-IR, and GPC (gel permeation chromatography). The composition number 25/50/75 was assigned based on the mol percent−feed ratio of the terthiophene present. For example, P3TC-25 is composed of 25 mol % of the terthiophene monomer feed ratio. The polymers were found to be readily soluble in common organic solvents such as $CHCl_3$, CH_2Cl_2, and THF. The composition of the copolymers was calculated by integrating the area under the peak of the carbazole proton signal (δ = 7.9 ppm) and the terthiophene proton signal (δ = 2.9 ppm,) as shown in Figure 1a. The percent fraction of carbazole (F_{CBZ}) in the copolymer can be determined using the following relationship:

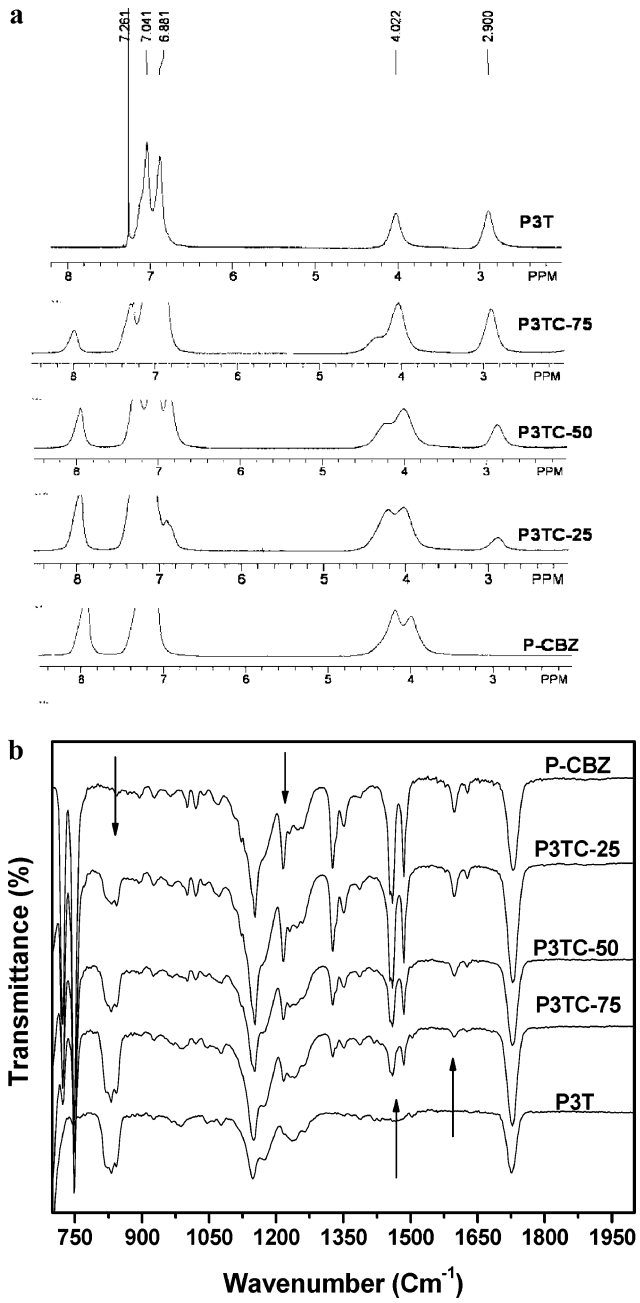

Figure 1. Characterization of precursor polymers using (a) NMR spectra and (b) FTIR spectra.

$$F_{CBZ}\,(\%) = \frac{2(\mathrm{CBZ})}{2(\mathrm{CBZ}) + 2(\mathrm{TT})} * 100$$

where CBZ and TT stand for the total peak areas of carbazole 3,6-position protons and protons from the methylene group substituted on terthiophene. On the basis of this equation, the percent F_{CBZ} for P3TC-25, P3TC-50, and P3TC-75 were found to be 81, 57, and 24%, respectively. The results are based on 5% error in NMR integration and 1% from the monomer feed ratio.

Table 1. Number-Average (M_n) and Weight-Average (M_w) Molecular Weights and PDI of the Polymers

precursor polymers	M_n	M_w	polydispersity (PDI) = M_w/M_n
P3T	52346	119653	2.28
P3TC-75	32256	70993	2.20
P3TC-50	67653	180153	2.66
P3TC-25	30416	84772	2.78
P-CBZ	29051	83318	2.86

The slight deviations in observed copolymer composition from its expected value may be due to the differences in the reactivity ratios of CBZ-A and 3T−A.

Figure 1b shows the comparative FTIR spectra of the synthesized precursor polymers. FTIR shows very distinct peaks from both carbazole and terthiophene, and the peak intensities vary on going from one polymer composition limit to the other. A very good correlation is observed in the peak intensities of the copolymer compositions and their respective homopolymers. As seen from Figure 1b, the terthiophene shows a strong characteristic out of plane broad vibrational peak between 817 and 839 cm^{-1} arising from $(C_\beta-H)_{ring}$ of the thiophene ring, while carbazole shows its characteristic peaks at 1217, 1460−1520, and 1590 corresponding to the $(C-N)_{ring}$, carbazole aromatic (C−H), and carbazole $(C=C)_{ring}$ vibrations, respectively.[15]

The molecular weights of the precursor polymers were determined using gel permeation chromatography (GPC) by dissolving them in THF and recording the molecular weight against PMMA standards. The molecular weights of the polymers are summarized in Table 1. Except for P3TC-75, all the polymers were found to have increasing PDI with increasing carbazole content.

Electropolymerization. The precursor polymers (homopolymer and copolymer) were electropolymerized and deposited on ITO substrates. The chemical structures of the cross-linked polymers are outlined in Scheme 2. The cyclic voltammetry (CV) curves are shown in Figure 2.

The electrochemical polymerization was performed using 5 mM each polymer solution in CH_2Cl_2 containing 0.1 M TBAP as an electrolyte. The potential was cycled from 0 V up to 1.2 V at a scan rate of 20 mV/s against Ag/AgCl as a reference and Pt as a counter electrode. The oxidation onset of the monomer was recorded in their anodic scan as shown in Figure 2a and Table 2. The difference of the oxidation onsets of the two homopolymers is ∼0.22 V. Since terthiophene has a slightly lower oxidation onset potential (monomer) as compared to carbazole, it is expected to initiate first (formation of radical cation) in any given copolymer composition, but the possibility of carbazole initiation along with the terthiophene cannot be discounted. Nevertheless, a very good trend of increasing oxidation onset potentials was observed in going from the P3T homopolymer to P−CBZ (Table 2). Such precisely tunable onset potentials are an advantage among these precursor polymers since it allows one to quantitatively observe the copolymerization between carbazole and terthiophene.

Table 2 shows the peak anodic/cathodic potentials of the cross-linked polymer after the seventh cycle. All the polymers were found to have an increasing trend in the anodic peak potential (E_{pa}) and a subsequent decrease in cathodic peak potential (E_{pc}) as a function of increasing terthiophene content with the exception of the P3TC-25 polymer. Similar trends were observed in both peak anodic currents (i_{pa}) and cathodic currents (i_{pc}) in the polymers. Figure 3 shows a linear fit observed for both $(i_{pa})/(i_{pc})$ as a function of polymer composition with again an exception

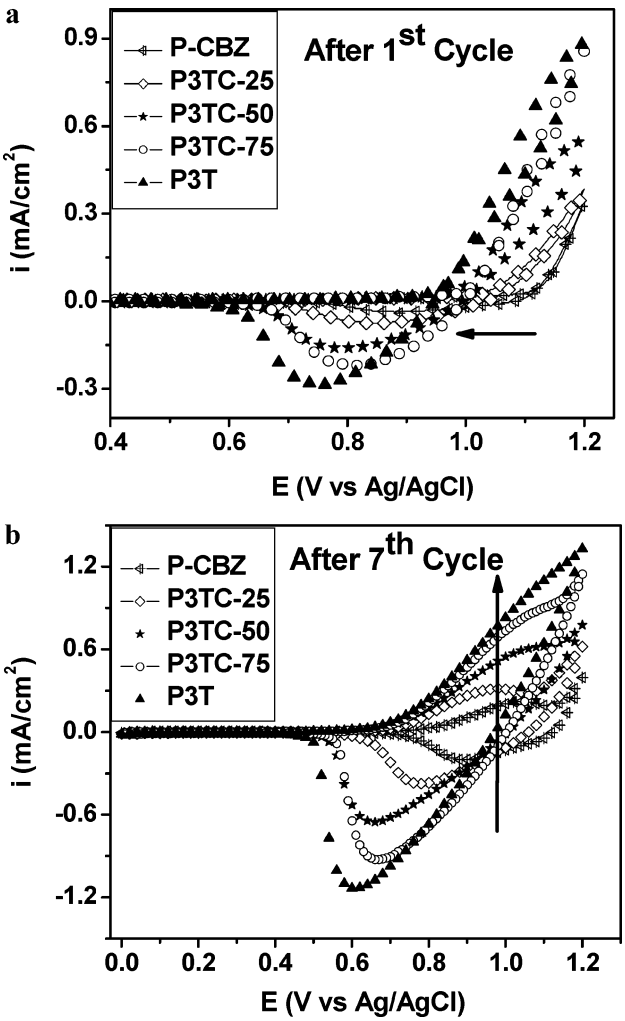

Figure 2. Comparative cyclic voltammograms of the polymers after (a) first cycle and (b) seventh cycle.

Table 2. Precursor Polymers Showing Peak Anodic and Cathodic Currents/Potentials and Their Corresponding Onsets of Oxidation Potential

precursor polymers	onsets	E_{pa} (V)	i_{pa} (mA)	E_{pc} (V)	i_{pc} (mA)
P3T	0.85	1.08	1.05	0.60	−1.14
P3TC-75	0.92	1.05	0.84	0.67	−0.93
P3TC-50	0.96	1.04	0.59	0.66	−0.66
P3TC-25	1.01	0.96	0.31	0.77	−0.36
P-CBZ	1.07	1.01	0.22	0.89	−0.19

for the P3TC-25 polymer. To further understand this trend, a spectro-electrochemical analysis was performed.

Spectro-electrochemical Studies. The in situ spectro-electrochemical studies performed under monomer free conditions are shown in Figure 4. The cross-linked precursor polymers were analyzed in a monomer free condition by applying a constant potential of 0 and 1.0 V. At 0 V, all the polymers were in their neutral form. The $\pi-\pi^*$ transition at 310 nm, a tailing absorption at 335 nm, which is attributed to polycarbazole[16] in CP−CBZ, and the polythiophene[17] peak at 432 nm corresponding to in CP3T are all observed in the spectra of Figure 4. However, a low energy polaron band was also seen at 424 nm in CP−CBZ, indicating incomplete neutralization of polycarbazole even after

(16) (a) Abe, Y.; Bernede, J.; Delvalle, A. M.; Tregouet, Y.; Diaz, R.; Lefrrant, S. *Synth. Met.* **2002**, *126*, 1−6. (b) Hayashida, S.; SukegawaOsamu, K. N. *Synth. Met.* **1990**, *35* (3), 253−261.

(17) Jang, S.-Y.; Sotzing, G. *Macromolecules* **2002**, *35*, 7293−7300.

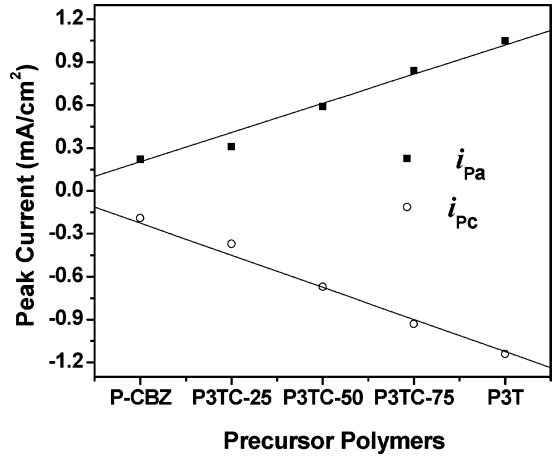

Figure 3. Variation of peak anodic and cathodic currents as a function of polymer composition.

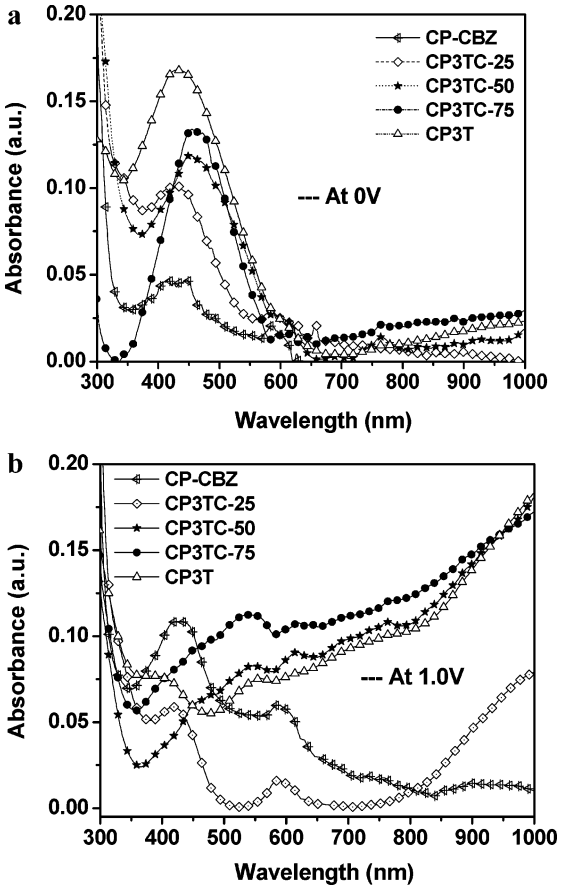

Figure 4. Spectro-electrochemical changes for the polymers at a constant voltage of 0 and 1.0 V.

the end of the seventh CV cycle. The fact that a high energy shoulder at 3.76 eV (335 nm) was observed together with the existence of polaronic peaks even after applying 0 V indicates a relatively poor homopolymer polycarbazole film formation.

In the case of electrochemically formed cross-linked copolymers, the absorption spectra were found to be very different from their corresponding cross-linked homopolymers. This could be due to a triggering effect wherein a lower oxidation potential electro-active unit triggers the polymerization of an electro-active unit having a relatively higher oxidation potential in a statistical binary mixture.[5] If this is true in the present case, then in principle, one should be able to successfully extend the polymerization of carbazole by itself or its involvement in the copolymerization with the terthiophene depending on its composition ratio.

In the case of CP3TC-25, two absorption peaks were observed at 352 nm (tailing) and 432 nm due to the extended $\pi-\pi^*$ conjugation of polycarbazole and polythiophene, respectively. Since both these peaks correspond to their respective homopolymers, and the fact that this composition contains mostly carbazole, the relative percentage of copolymerization between thiophene and carbazole is difficult to estimate. However, CP3TC-25 shows the extended $\pi-\pi^*$ transition of polycarbazole, as compared to CP−CBZ, suggesting that the presence of the terthiophene is triggering more polymerization of carbazole in this case. This extended $\pi-\pi^*$ conjugation of polycarbazole in cross-linked P3TC-25 also explains the slight anomaly in the trend of E_{pa} (V) observed during cyclic voltammetry.

Furthermore, this triggering effect is more clearly seen in CP3TC-50, where a higher percentage of terthiophene is involved as compared to CP3TC-25. Since this composition is an equimixture of both electro-active groups, the possibility of the copolymerization extent should be higher. P3TC-50 shows an absorption peak at 350 nm due to carbazole homopolymerization along with a new low energy absorption peak at 450 nm (Figure 4a), which could be due to the copolymerization of terthiophene and carbazole. However, the possibility of terthiophene polymerization by itself cannot be ignored, and a high possibility exists that the peak observed at 432 nm due to polythiophene is well-masked under the newly formed peak. We also observed a new peak at 458 nm for P3TC-75, with almost no absorption peak due to polycarbazole, indicating that almost all the carbazole is involved in the copolymerization. From these results, it can be concluded that based primarily upon the terthiophene content, the initiation eventually prefers the formation of either an extended carbazole homopolymerization or an efficient copolymerization.

Figure 4b shows the UV−vis spectra of the different polymer ratios at 1.0 V, which allows one to specifically see the absorption due to the charged doped state of the conjugated polymer. The homopolymer and copolymers with different compositions will have their unique low energy doped state signatures and therefore could be used to distinguish from the copolymers. Because of the absorption of the low energy charged state, the absorption in the visible range due to the $\pi-\pi^*$ transition bleaches.[5,18] In CP−CBZ, at 1.0 V, the peak due to the $\pi-\pi^*$ transition at 310 nm bleaches and shows a chromic shift from colorless to green, giving rise to two new peaks at 424 and 605 nm (Figure 4b). The peaks at 424 and 605 nm have been understood to arise from the polaron bonding level to the π^* conduction band and bonding level to antibonding state of polaron transitions, respectively.[19] The cross-linked homopolymer CP3T shows a quenching in the $\pi-\pi^*$ transition at 432 nm, and a new peak arises at 800 nm, attributed to the π to bipolaron transition.[7a,17]

The CP3TC-25 composition shows three distinct charged peaks (424, 605, and 800 nm) (Figure 4b), indicating that this composition primarily consist of a combination of both homopolymers. The polymer CP3TC-50 and CP3TC-75 both show quenching of their respective $\pi-\pi^*$ transitions, and a new peak appears at 550 nm in the case of CP3TC-50, while the polymer CP3TC-75 shows its new peaks at 538 nm arising due to the varying extent of copolymerization between thiophene and carbazole.[20] Both the compositions of CP3TC-50/CP3TC-75 also show peaks due to polythiophene π to bipolaron transitions above 800 nm. Although the copolymerization peaks are ill-defined

(18) Baba, A.; Knoll, W. *J. Phys. Chem. B* **2003**, *107*, 7733−7738.
(19) (a) Kessel, R.; Schultz, W. J. *Surf. Interface Anal.* **1990**, *16*, 401−406. (b) Varghese, M. M.; Basu, T.; Malhotra, B. D. *Mater. Sci. Eng., C* **1995**, *3*, 215−218.
(20) Zotti, G.; Schiavon, G.; Zecchin, S.; Morin, J. F.; Leclerc, M. *Macromolecules* **2002**, *35*, 2122−2128.

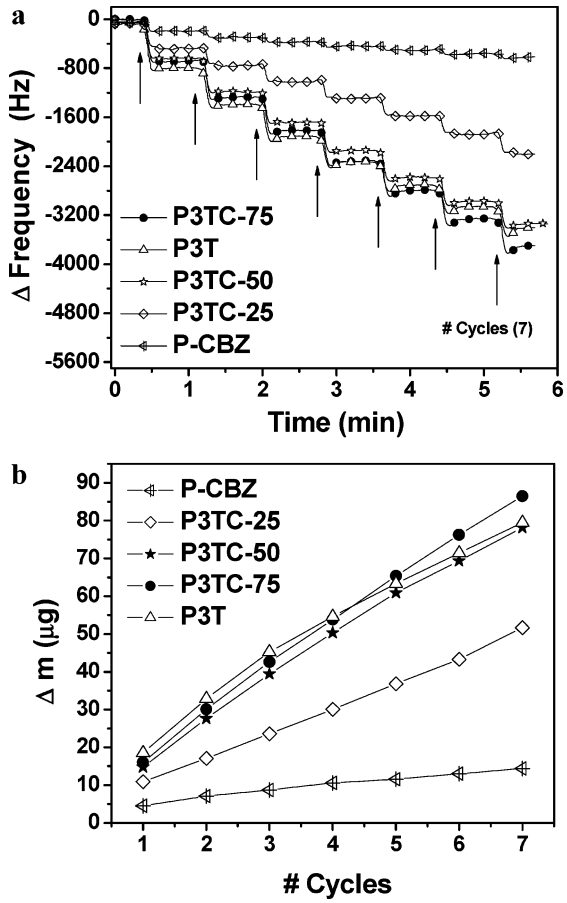

Figure 5. EC-QCM results: (a) frequency change as a function of time and (b) change in mass Δ*m* as a function of CV cycles.

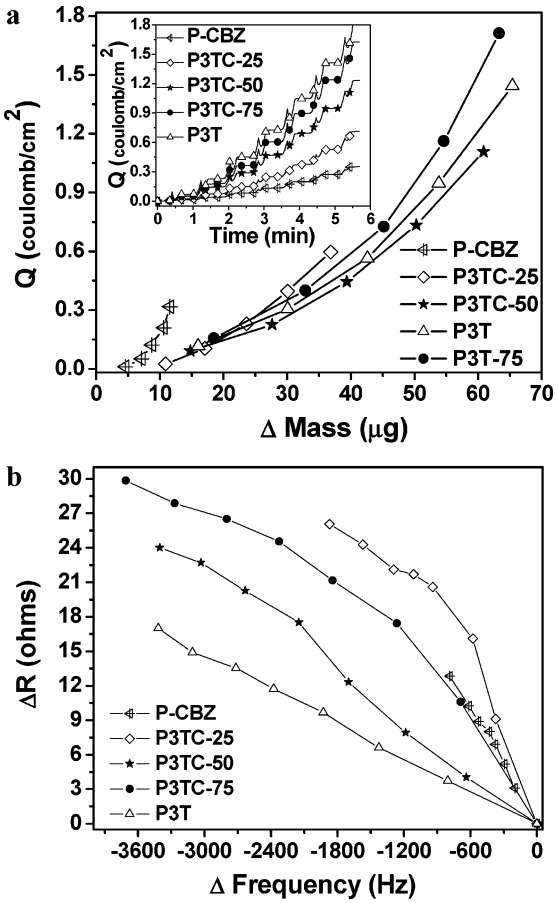

Figure 6. EC-QCM results: (a) efficiency of polymerization and inset showing the amount of charge (*Q*) during the electrodeposition. (b) Changes in the viscoelastic behavior in the polymers.

and it is hard to judge the extent of copolymerization, the absence of distinct peaks due to the carbazole homopolymer clearly indicates that carbazole is involved mostly in the copolymerization unlike the case of CP3TC-25. It should be noted that the distribution of the terthiophene, which is assumed to be statistical, may also play an important role since the cross-linking phenomena is a consequence of intra- and intermolecular reactions.

EC-QCM. The combination of the QCM technique with electrochemical methods has made possible in situ measurements of minute mass changes that take place during adsorption, under potential deposition, under dissolution of surface films, and other electrochemical processes.[21] In most of these investigations, frequency changes (Δ*F*) were interpreted in terms of rigid mass changes, based on the Sauerbrey equation.[22] For thin films (where the film thickness is much less than the wavelength of the piezoelectrically launched shear waves), a modified Sauerbrey equation is used to convert Δ*F* to mass changes (Δ*m*) as reported by Baba et al.[23] Figure 5a shows a periodic change in Δ*F* on the working electrode during the formation of the cross-linked polymer films as a function of time.

A corresponding increase in the Δ*m* (Figure 5b) is indicative of the growth of an electrochemically active thin film. Figure 5b shows a clearer picture, where the periodic change of mass is seen as a function of CV cycles. The polymer P−CBZ shows the lowest Δ*m* value, suggesting a relatively poor polymer growth of its cross-linked form (CP−CBZ) on the electrode as also suggested in the spectro-electrochemical studies. But with an increasing terthiophene content, the extent of involvement of the carbazole increases. This can be clearly seen by comparing the Δ*m* values of the P3TC-25, P3TC-50, and P3TC-75 precursor copolymers to the P3T homopolymer. The P3T homopolymer deviates slightly from its linearity in a mass change after the fourth cycle. On the other hand, P3TC-75 shows a very linear growth and the highest change in Δ*m* value. This indicates that the carbazole is primarily involved in the copolymerization, leading to a more uniform growth and higher joint mass. P3TC-50 follows similar trends. P3TC-25 shows significant enhancement in Δ*m* values as compared to that of P−CBZ, indicating a thick film of polycarbazole, due to an intervention of terthiophene as an initiator. What is important to note is that beginning with P3TC-50, the Δ*F* and Δ*m* values are nearly the same for P3TC-75 and P−CBZ, indicating that most of the carbazole units have been incorporated in the copolymer already. These results support the spectro-electrochemistry observations described earlier and are confirmed with further discussion of the results.

The polymerization efficiency of the precursor polymers can be seen from Figure 6a, which shows the changes in amount of charge (*Q*) as a function of mass deposition during electrochemical polymerization. The polymer P3TC-50 shows the highest polymerization efficiency, while the P−CBZ precursor polymer is the lowest. In the case of P3TC-75, where only ∼25% of carbazole is present, the efficiency was found to be just slightly lower than that of the P3T homopolymer. These results indicate that the efficiency of copolymerization especially in the case of

(21) Buttry, D. A. In *Electroanalytical Chemistry*; Bard, A. J., Ed.; Marcel Dekker: New York 1991; Vol. 17, p 1.
(22) Sauerbrey, G. *Phys. Z.* **1959**, *155*, 206−212.
(23) (a) Baba, A.; Tian, S.; Stefani, F.; Xia, C.; Wang, Z.; Advincula, R.; Johannsmann, D.; Knoll, W. *J. Electroanal. Chem.* **2004**, *562*, 95−103 (b) Baba, A.; Kaneko, F.; Advincula, R. C. *Colloids Surf., A* **2000**, *173*, 39−49.

the 50% composition is most prominent, where the chances or extent of equal copolymerization is expected to be the highest. The Figure 6a inset shows that all the polymers have a linear change of charge as a function of time and indicates the extent of cross-linking that is occurring during the electropolymerization.

The copolymerization behavior was further probed by analyzing the changes in the viscoelastic properties during the cross-linking polymerization. The Sauerbrey equation alone does not account for viscous losses or viscoelastic effects; therefore, it was necessary to use a modified form, which also accounts for the acoustic impedance of the film. In air, such viscoelastic effects scale as the cube of the film thickness and can be neglected, but in liquids, this is not the case because liquids exerts a lateral stress on the depositing upper surface of the film. The resulting viscous coupling of the solution with the film effectively adds a mass component to the oscillating crystal. Hence, when the QCM operates under inelastic conditions, it becomes difficult to differentiate contributions attributed to the bound mass from that of the solution viscosity to the total change in frequency. In this case, impedance analysis of the QCM resonator has proven to be effective in providing additional information on the solid/liquid interface.[24]

This analysis is based on the well-known Butterworth−van Dyke (BD) equivalent circuit that provides the structure for relating the electrical properties of the quartz resonator to the mechanical properties of the deposited film.[25] In this regard, the BD circuit element R (motional resistance) is useful in probing the energy loss or dissipation factor (D) due to the dampening process that occurs in viscoelastic systems.[26] The relationship between ΔR and Δf under liquid loading is given by the equation[27]

$$\Delta R = (2\pi f \rho_L \eta_L)^{1/2} A_r / k^2$$

where, ΔR is the change in resonance resistance in Ω (ohms); A_r is the active crystal area; k is the electromechanical coupling factor; f is the resonant frequency of unloaded crystal in hertz; ρ_L is the density of quartz (2.648×10^3 kg/m^3); and η_L is the liquid viscosity in contact with the electrode in N s/m^2. Thus, an increase in ΔR is correlated with an increase in the viscoelasticity of the layer adjacent to the crystal surface while a small change in ΔR is indicative of a more rigid adsorbed layer. While it is true that viscoelastic effects play a role in frequency changes when characterized by EC-QCM, in principle, we can correlate the viscoelastic change as a function of composition during the cross-linking of the polymers.

During the anodic cycle, the film is deposited along with the doping of ions, and the doping of ions makes the film more rigid in nature; therefore, ΔR decreases. But during the cathodic cycle, the change is specifically due to de-doping as the deposited film remains and becomes neutralized. Figure 6b shows a thickness independent comparative graph between ΔR and Δf for different polymers. A huge change in viscoelastic properties is observed during de-doping, and this change varies on going from the homopolymer to the different copolymer compositions based upon their extent of copolymerization. The slope of ΔR was found to be highest in the case of P−CBZ and lowest for P3T. The polymer P3TC-25 initially shows ΔR changes similar to that of polycarbazole and later ends up in behaving more like polythiophene in character, which indicates no or little copolymerization character. On the other hand, P3TC-50 initially behaves more like polythiophene but starts to deviate from the third CV cycle, which probably is an indication of carbazole involvement. Finally, P3TC-75 begins to show a very different ΔR behavior from either of the homopolymers, which may be due to an early copolymerization but later behaves more like polythiophene. This is reasonable because if most of the carbazole units are already consumed, then only terthiophene is left to polymerize. These results also indicate the involvement of a triggering effect of terthiophene toward initiating the carbazole polymerization.

EC−SPR. A comparative analysis of the two homopolymers (P3T/P−CBZ) and copolymer (P3TC-50) was performed to confirm the effective deposition (growth kinetics of the copolymerization film) and electrochromic effect among these polymers. We measured the electrochemical/optical properties by simultaneous EC−SPR.[28] Figure 7a shows SPS electrodeposition kinetic curves for (1 mM) polymer dissolved in CH_2Cl_2 solution containing 0.1 M TBAP. The data were recorded as a function of time (up to 3.5 cycles). Figure 7a shows that reflectivity increases in all the compositions, indicating the deposition of the film onto the Au substrates by potential cycling. As expected during the CV, the SPR curves show that the film thickness increases with increasing ratio of P3T, indicating the influence of the P3T precursor toward forming a thicker film.

The chromic effect is a consequence of both doping and de-doping processes, and the extent of chromic changes can be measured and compared in terms of the reflectivity changes (ΔR) within these polymers. The polymer P3T shows significant electrochromic effects in going from colorless at 0 V to reddish-orange at 1.0 V and greenish-blue at 0.8 V. The polymer P−CBZ is colorless at 0 and 0.8 V but turns green at 1.0 V. Besides, in the stepwise increase of the reflectivity, a large reflectivity alteration was observed in the case of P3T as shown in Figure 7a. The alteration was observed at the onset potential of doping (∼0.8 V in anodic scan) and of de-doping (∼0.6 V in cathodic scan), indicating that the dielectric constant of the P3T film changed drastically upon doping−de-doping. On the other hand, a little alteration of reflectivity was observed by doping−de-doping in the case of P−CBZ. This corresponds to the simultaneous observation of the amount of charge (i.e., a little charge transfer was observed by doping−de-doping in P−CBZ). In the case of the copolymer, the change of the reflectivity was between P3T and P−CBZ, indicating that P3T plays a main role in the change of the dielectric constants. The de-doping efficiency indicates a change of dielectric constant in the film and is co-related with the electrochromic effect within the films.[29]

Table 3 shows the efficiency of these changes during the deposition of the film. During de-doping, the efficiencies were found to be 17.4, 10.5, and 3.29 for P3T, P3TC-50, and P−CBZ, respectively. These values indicate that the film containing P3T has the largest electrochromic property, which can also be seen in the kinetic measurement during the electropolymerization. The reflectivity changes could not be observed beyond the third cycle because of the huge change in reflectivity and thickness of the P3T film saturating the SPS signals.

After the electropolymerization, the films were rinsed with CH_2Cl_2, and then they were measured in monomer free acetonitrile solution containing 0.1 M TBAP. Figure 7b show the angular

(24) (a) Kanazawa, K. *Faraday Discuss.* **1997**, *107*, 77−90. (b) Etchenique, R.; Buhse, T. *Analyst* **2000**, *125*, 785−787.
(25) Buttry, D. A.; Ward, M. D. *Chem. Rev.* **1992**, *92*, 1355−1379.
(26) Geelhood, S. J.; Frank, C. W.; Kanazawa, K. *J. Electrochem. Soc.* **2002**, *149*, 33−38.
(27) Muramatsu, H.; Tamiya, E.; Karube, I. *Anal. Chem.* **1988**, *60*, 2142−2146.
(28) Baba, A.; Advincula, R. C.; Knoll, W. *J. Phys. Chem. B* **2002**, *106*, 1581−1587.
(29) (a) Baba, A.; Park, M.-K.; Advincula, R. C.; Knoll, W. *Langmuir* **2002**, *18*, 4648−4652. (b) Baba, A.; Lübben, J.; Tamada, K.; Knoll, W. *Langmuir* **2003**, *19*, 9058−9064.

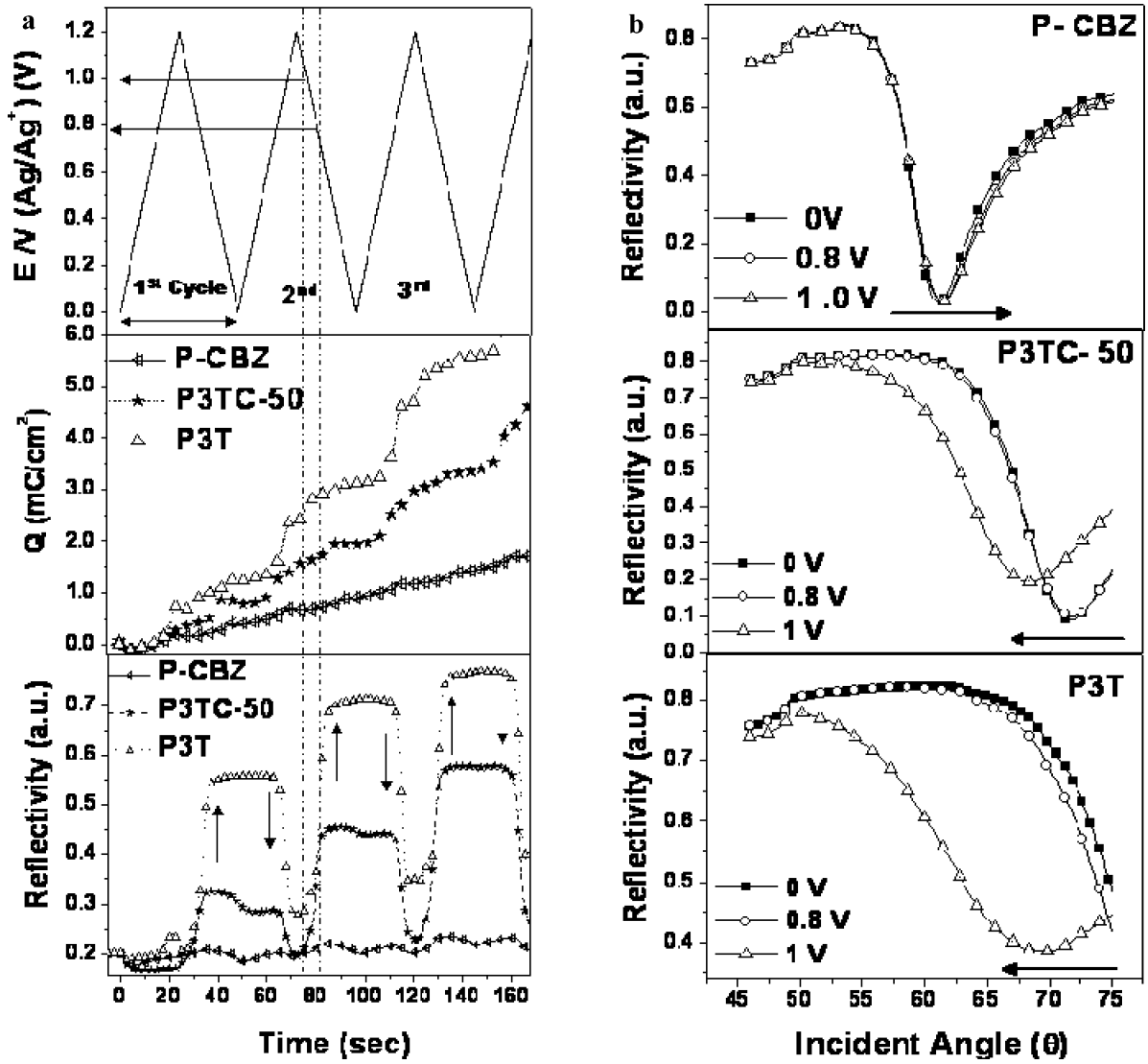

Figure 7. EC-SPR results: (a) potential ramp and SPR kinetic curve during electrodeposition of P3T/P3TC-50/P-CBZ in 0.1 M TBAP and (b) angular curves obtained in monomer free acetonitrile containing 0.1 M TBAP solution for the electrodeposited polymers.

Table 3. Reflectivity Change (d*R*) and Amount of Charge (*Q*) during Electrodeposition and Current Efficiency after Two Potential Cycles

	P3T		P3TC-50		P-CBZ	
	doping	de-doping	doping	de-doping	doping	de-doping
reflectivity change (d*R*)	0.11	0.53	0.03	0.21	0.02	0.03
Q (mC/cm^2)	2.32	3.03	1.45	1.99	0.69	0.91
efficiency (d*R*/d*Q*)100	4.74	17.4	2.06	10.5	2.90	3.29

SPR curves under constant potential applied to investigate doping−de-doping properties of deposited thin films. It is very clear from Figure 7b that P3T shows a huge change in the incident angle as well as reflectivity during doping−de-doping. These simultaneous changes occur due to the changes in the real (ϵ) and imaginary parts ($\acute{\epsilon}$) of the dielectric constant along the conjugated polymer backbone.[8] The change in thickness of the film should also have a contribution. In the case of P3TC-50, an intermediate change was observed, and almost no change was seen for P−CBZ. In the case of P3TC-50, both efficiency and angle show an intermediate change, which suggests that this change is due to an effective copolymerization but that the reflectivity is mainly due to the properties of the polythiophene. The results obtained from EC-QCM and spectro-electrochemistry also support this observation.

Conclusion

In summary, five different polymers were synthesized for a precursor polymer approach based on binary composition of two different pendant electro-active groups (terthiophene and carbazole) onto a polymethacrylate (PMMA) polymer backbone. A comparative analysis was performed to investigate the electrochemical copolymerization behavior between terthiophene and carbazole as compared to their homopolymer analogues. The terthiophene was found to trigger the polymerization of carbazole either to generate extended conjugation in polycarbazole or increase its involvement in copolymerization. The extent of copolymerization was found to be highly dependent on the terthiophene composition and is considered a limiting step. Thus, P3TC-25 shows mainly the formation of polycarbazole, while P3TC-50 shows a higher copolymerization extent. Finally, the

P3TC-75 composition ratio shows a complete involvement or consumption of carbazole units in the copolymer that then progressively incorporates the polythiophenes. The role of the terthiophene, which has a slightly lower oxidation potential, essentially triggers the polymerization of the carbazole that by itself is not very efficient in forming a homopolymer. On the other hand, by generating the radical cations first through the terhiophenes, the polymerization of carbazole (homopolymer and copolymer) becomes more efficient. These results provide a unique insight to the electrocopolymerization phenomena and at the same time provides a materials synthesis protocol for functional electrochromic films useful for device or sensing applications.

Acknowledgment. The authors gratefully acknowledge the partial funding from the Robert A. Welch Foundation (E-1551), NSF DMR-0504435, DMR-0602896, and DMR-99-82010. We also acknowledge technical support from Varian Inc., Viscotek Inc., and Maxtek Inc.

LA061820D